# Peristaltic Transport of aCouple-Stress Fluidwith Nanoparticles in an Inclined Tube

K. Maruthi Prasad[1], N. Subadra[2], U. S. Mahabaleshwar[3]

*1Department of Mathematics, School of Technology, GITAM University, Hyderabad 502329, Telangana, India*
*[2]Department of Mathematics, Geethanjali College of Engg.and Tech., Cheeryal (V), Keesara (M), R. R. Dist. 501301, Telangana, India*
*[3]Department of Mathematics, Government First Grade for Women, Hassan, 573201,Karanataka,India*

***Abstract****: The paper deals with a theoretical investigation of the peristaltic transport of a couple-stress fluid with heat and mass transfer effects. The velocity, pressure drop, time averaged flux, frictional force, mechanical efficiency, temperature profile, nano particle phenomena, heat transfer coefficient and mass transfer coefficient of the fluid are investigated, when the Reynolds number is small and wave length is large by using appropriate analytical methods. Effects of different physical parameters like couple-stress fluid parameters, Brownian motion parameter, thermophoresis parameter, local temperature Grashof number as well as local nano particle Grashof number on pressure drop characteristics, frictional force, heat transfer coefficient, mass transfer coefficient and steam line patterns of the fluid are studied.The expressions for velocity, temperature profile, nano particle phenomenon, heat transfer coefficient and mass transfer coefficients are sketched through graphs. The streamlines are drawn to discuss trapping phenomenon for some physical quantities.*

**Keywords:***Peristalsis, Couple-stress fluid, Brownian motion parameter, Thermophoresis parameter, Mechanical Efficiency, Heat transfer coefficient, Mass transfer coefficient*.

## 1. Introduction

Peristaltic pumping is a word used to describe a progressive wave of contraction along a tube whose cross-sectional area consequently changes. Peristalsis is an inherent property of many tabular organs of the human body. The mechanism of peristaltic transport has been exploited for industrial applications like sanitary fluid transport, blood pumps in the heart lung ma chine, transport of corrosive fluids. In view of its importance, a number of researchers investigated peristaltic transport of Newtonian and non-Newtonian fluids under different conditions (Fung & Yih, (1968), Shapiro et al. (1969), Griffiths, (1989), Srinivasacharya et al. (2003), Prasad, Radhakrishnamacharya, & Murthy, (2010), Ellahi et al. (2014), Prasad et al. (2015)).

Couple-stress fluid model has been widely used by researchers because of its relative mathematical simplicity compared with other models. Blood, lubricants containing small amount of high polymer additives, electro-rheological fluids and synthetic fluids show the effect of couple-stress and rotation of molecules, which are not present in the case of Newtonian fluids. Hence couple-stress fluid serves as a better model for these fluids. Couple-stress fluids was developed by Stokes, (1966). Pal et al. (1988) studied and developed a couple stress model of blood flow in the microcirculation. Effect of peripheral layer on peristaltic transport of a couple-stress fluid was investigated by Prasad & Radhakrishnamacharya, (2009). Maiti & Misra, (2012) studied peristaltic transport of a couple stress fluid: some applications to hemodynamics. Hydromagnetic effect on inclined peristaltic flow of a couple stress fluid was developed by Shit & Roy, (2014).

Nanotechnology has immense contribution in industry since materials of nanometer dimensions exhibit incomparable physical and chemical characteristics. Water, ethylene glycol and oil are common examples of base fluids used for the nanofluid phenomena. Nanofluids have their enormous applications in heat transfer, such as microelectronics, fuel cells, pharmaceutical processes and hybrid powered engines. They explore enhanced thermal conductivity. A large amount of literature is available which deals with the study of nanofluid and its applications. S. U.S. Choi, (1995) was the pioneer to study the nanofluids. Pool boiling of nano-fluids on horizontal narrow tubes was studied by Das et al. (2003). Noreen, (2013) investigated mixed convection peristaltic flow of third order nanofluid with an induced magnetic field. Study of peristaltic motion of nanoparticles of a micropolar fluid with heat and mass transfer effect in an inclined tube was done by Prasad et al. (2015).

It is known that many ducts in physiological system are not horizontal but have some inclination with the axis. Slip effects on peristaltic transport of power-law fluid through an inclined tube was investigated by Naby & Shamy, (2007). Maruthi Prasad & Radhakrishnamacharya, (2008) studied flow of Herschel–Bulkley fluid through an inclined tube of non-uniform cross-section with multiple Stenoses. Shit & Roy, (2014) discussed Hydromagnetic effect on inclined peristaltic flow of a couple -stress fluid. Peristaltic transport of a nanofluid in an inclined tube was investigated by Prasad et al. (2015).

Keeping all the above in view, peristaltic transport of a couple-stress fluid with nanoparticles in an inclined tube has been investigated under the

assumption of long wavelength and low Reynolds number. The coupled equations of temperature profile and nanoparticle phenomena have been solved by using homotopy perturbation method. The analytical solutions of pressure drop, velocity, frictional force, temperature profile and nanoparticle phenomena are obtained. The effects of various parameters on these flow variables have been depicted through graphs.

## 2. Mathematical Formulation

Consider the peristaltic transport of an incompressible couple stress fluid with nanoparticles in atube of uniform cross section of radius '$a$' with sinusoidal wave travelling along the boundary of the tube with speed $c$, amplitude $b$ and wave length$\lambda$.Further the tube is inclined at an angle $\alpha$ with the horizontal axis. Choosing the cylindrical polar coordinate system $(R, \theta, Z)$, the wall deformation due to the propagation of an infinite train of peristaltic waves is given by

$$R = H(z,t) = a + bSin\frac{2\pi}{\lambda}(Z - ct) \quad (1)$$

The governing equations in the fixed frame for an incompressible couple-stress fluid flow with nanoparticlesin the absence of body moment and body couple are given as (Maiti et al.,(2012))

$$T_{ji\,,j} = \rho\frac{dw_i}{dt} \quad (2)$$

$$e_{ijk}\,T^A_{jk} + M_{ji\,,j} = 0 \quad (3)$$

$$l_{ij} = -p\delta_{ij} + 2\mu_{ij}\,d_{ij} \quad (4)$$

$$\mu_{ij} = 4\eta\omega_{j\,,i} + 4\eta'\omega_{ij} \quad (5)$$

$$(\rho c)_f\frac{dT'}{dt} = k\nabla^2 T' + (\rho c)_p[D_B\nabla C'.\nabla T' + \frac{D_T}{T_0}\nabla T'.\nabla T'] \quad (6)$$

$$\frac{dC'}{dt} = D_B\nabla^2 C' + \left[\frac{D_T}{T_0}\right]\nabla^2 T' \quad (7)$$

where $w_i$ is the velocity vector, $T_{ij}$ and $T^A_{ij}$ are the symmetric and antisymmetric parts of the tensor $T_{ij}$ respectively, $M_{ij}$ is the couple-stress tensor, $\mu_{ij}$ is the deviatoric part of$M_{ij}$, $\omega_{ij}$ is the vorticity vector, $d_{ij}$ is the symmetric part of the velocity gradient, $\eta$ and $\eta'$ are constants associated with the couple-stress, $p$ is the pressure and other terms have their usual meaning from tensor analysis.$\rho_f$is the density of the fluid, $\rho_p$ is the density of the particle, $C$ is the volumetric volume expansion coefficient, $f$ represents the body forces, $\frac{d}{dt}$represents the material time derivative, $\bar{C}$is the nano particle concentration, $D_B$is the Brownian diffusion coefficient and $D_{\bar{T}}$is the thermophoretic diffusion coefficient. The ambient values of $\bar{T} and \bar{C}$ as $\bar{r}$ tend to $\bar{h}$ are denoted by $\overline{T_o}$and $\overline{C_o}$ .

Using the transformation

$r = R, z = Z - ct, u = U, w = W - c, \theta = \theta$

From a stationary to a moving frame of reference, the equations (2) – (7) are converted to

$$\mu\nabla^2\left[1 - \frac{1}{\bar{\alpha}^2}\nabla^2\right]w' = \frac{dp'}{dz'} + \rho g\beta(T' - T_0') + \rho g\beta(C' - C_0') - \frac{\cos\alpha}{F} \quad (8)$$

$$\left[u'\frac{\partial T'}{\partial r'} + w'\frac{\partial T'}{\partial z'}\right] = \beta\left[\frac{\partial^2 T'}{\partial r'^2} + \frac{1}{r'}\frac{\partial T'}{\partial r'} + \frac{\partial^2 T'}{\partial z'^2}\right] + \tau\left\{D_B\left[\frac{\partial C'}{\partial r'}\frac{\partial T'}{\partial r'} + \frac{\partial C'}{\partial z'}\frac{\partial T'}{\partial z'}\right] + \frac{D_T'}{T_0'}\left[(\frac{\partial T'}{\partial r'})^2 + (\frac{\partial T'}{\partial z'})^2\right]\right\} \quad (9)$$

$$\left[u'\frac{\partial C'}{\partial r'} + w'\frac{\partial C'}{\partial z'}\right] = D_B\left[\frac{\partial^2 C'}{\partial r'^2} + \frac{1}{r'}\frac{\partial C'}{\partial r'} + \frac{\partial^2 C'}{\partial z'^2}\right] + \frac{D_T'}{T_0'}\left[\frac{\partial^2 T'}{\partial r'^2} + \frac{1}{r'}\frac{\partial T'}{\partial r'} + \frac{\partial^2 T'}{\partial z'^2}\right] \quad (10)$$

with$\nabla^2 = \frac{1}{r}\frac{\partial}{\partial r}\left(r\frac{\partial}{\partial r}\right)$

where$\tau = \frac{(\rho C)_p}{(\rho C)_f}$is the ratio between the effective heat capacity of the nanoparticle material and heat capacity of the fluid.

Introducing the following non-dimensional quantities:

$$r = \frac{r'}{a}, \quad z = \frac{z'}{\lambda}, \quad w = \frac{w'}{c}, \quad p = \frac{a^2 p'}{\lambda c\mu},$$

$$t = \frac{ct'}{\lambda}, u = \frac{\lambda u'}{ac}, \theta_t = \frac{T' - T_0'}{T_0'},$$

$$\delta = \frac{a}{\lambda}, R_e = \frac{2\rho ca}{\mu}, \quad \sigma = \frac{C' - C_0'}{C_0'},$$

$$\beta = \frac{k}{(\rho c)_f}, N_b = \frac{(\rho c)_p D_B C_0'}{(\rho c)_f},$$

$$N_t = \frac{(\rho c)_p D_T' T_0'}{(\rho c)_f \beta}, \quad G_r = \frac{g\beta a^3 T_0'}{\gamma^2},$$

$$B_r = \frac{g\beta a^3 C_0'}{\gamma^2},$$

$$\bar{\alpha} = a\alpha = \sqrt{\frac{\mu}{\eta}}a, \quad h' = \frac{h}{a}$$

Using the non-dimensional quantities in equations (8)-(10) and applying the long wavelength and low Reynolds number approximations and neglecting the inertial terms, the equations (8)-(10) are converted to

$$\frac{1}{r}\frac{\partial}{\partial r}\left(r\frac{\partial}{\partial r}\left(1 - \frac{1}{\bar{\alpha}^2}\nabla^2\right)w\right) = \frac{dp}{dz} + G_r\theta_t + B_r\sigma - \frac{\cos\alpha}{F} \quad (11)$$

$$0 = \frac{1}{r}\frac{\partial}{\partial r}\left(r\frac{\partial\theta_t}{\partial r}\right) + N_b\frac{\partial\sigma}{\partial r}\frac{\partial\theta_t}{\partial r} + N_t\left(\frac{\partial\theta_t}{\partial r}\right)^2 \quad (12)$$

$$0 = \frac{1}{r}\frac{\partial}{\partial r}\left(r\frac{\partial\sigma}{\partial r}\right) + \frac{N_t}{N_b}\left(\frac{1}{r}\frac{\partial}{\partial r}\left(r\frac{\partial\theta_t}{\partial r}\right)\right) \quad (13)$$

where $N_b, N_t, G_r, B_r$ are the Brownian motion parameter, Thermophoresis parameter, local temperature Grashof number and local nano particle Grashof number, and $w$ is the axial velocity, $r$ is the

radial coordinate, $\bar{\alpha}$ is the couple-stress fluid parameter, $\theta_t$ is the temperature profile and $\sigma$ is the nano particle phenomenon.

The non-dimensional boundary conditions are:

$$\frac{\partial w}{\partial r}=0,\ \frac{\partial \theta_t}{\partial r}=0,\ \frac{\partial \sigma}{\partial r}=0\ atr=0 \quad (14)$$

$$w=-1,\ \theta_t=0,\ \sigma=0\ \ atr=h(z)=1+\varepsilon sin2\pi z \quad (15)$$

$$\frac{\partial^2 w}{\partial r^2}-\frac{\overline{\eta}}{r}\frac{\partial w}{\partial r}=0\ \ atr=h(z)=1+\varepsilon sin2\pi z \quad (16)$$

$$\frac{\partial^2 w}{\partial r^2}-\frac{\overline{\eta}}{r}\frac{\partial w}{\partial r}\ is finite atr=0. \quad (17)$$

where $\varepsilon(=\frac{b}{a})$ is the amplitude ratio and $\eta'=\frac{\overline{\eta}}{\eta}$ is a couple-stress fluid parameter.

Boundary conditions (16) and (17) indicate that the couple-stresses vanish at the tube wall and is finite at the tube axis respectively.

## 3. Solutionof the Problem

Homotopy perturbation method is a combination of homotopy method and perturbation method. Homotopy perturbation method is more appropriate method than the other traditional perturbation methods. By using this method we will overcome the drawbacks of the traditional perturbation methods.

The homotopy for the equations (12) and (13) are as followsAkbar & Nadeem, (2013):

$$H(\zeta,\theta_t)=(1-\zeta)\left[L(\theta_t)-L(\theta_{t\,10})\right]+\zeta\left[L(\theta_t)+N_b\frac{\partial\sigma}{\partial r}\frac{\partial\theta_t}{\partial r}+N_t\left(\frac{\partial\theta_t}{\partial r}\right)^2\right] \quad (18)$$

$$H(\zeta,\sigma)=(1-\zeta)[L(\sigma)-L(\sigma_{10})]+\zeta\left[L(\sigma)+\frac{N_t}{N_b}\left(\frac{1}{r}\frac{\partial}{\partial r}\left(r\frac{\partial\theta_t}{\partial r}\right)\right)\right] \quad (19)$$

where $L=\frac{1}{r}\frac{\partial}{\partial r}\left(r\frac{\partial}{\partial r}\right)$ is taken as linear operator for convenience.

$$\theta_{t\,10}(r,z)=\left(\frac{r^2-h^2}{4}\right),\ \ \sigma_{10}(r,z)=-\left(\frac{r^2-h^2}{4}\right)\left(\frac{N_t}{N_b}\right) \quad (20)$$

are defined as initial guesses which satisfy the boundary conditions.

Define

$$\theta_t(r,z)=\theta_{t\,0}+\zeta\theta_{t\,1}+\zeta^2\theta_{t\,2}+\ ----- \quad (21)$$

$$\sigma(r,z)=\sigma_0+\zeta\sigma_1+\zeta^2\sigma_2+\ ---- \quad (22)$$

The series (21) and (22) are convergent for most of the cases. The convergent rate depends on the nonlinear part of the equation.

Adopting the same procedure as done by Akbar & Nadeem, (2013), the solution for temperature profile and nano particle phenomena can be written for $\zeta=1$ as

$$\theta_t(r,z)=N_t\left(\frac{r^3-h^3}{18}\right)-(N_b+N_t)\left(\frac{r^4-h^4}{64}\right)+N_bN_t\left(\frac{r^5-h^5}{300}\right)-N_bN_t\left(\frac{r^6-h^6}{1152}\right) \quad (23)$$

$$\sigma(r,z)=-\left(\frac{r^2-h^2}{4}\right)\frac{N_t}{N_b}+\left(\frac{r^2-h^2}{4}\right)\frac{N_t}{N_b}-\frac{{N_t}^2}{N_b}\left(\frac{r^3-h^3}{18}\right)+\frac{{N_t}^2}{N_b}\left(\frac{r^4-h^4}{64}\right) \quad (24)$$

Substituting Eqs. (23) and (24) in Eq. (11), it can be written as

$$\begin{aligned}\frac{1}{r}\frac{\partial}{\partial r}\left(r\frac{\partial}{\partial r}\left(1-\frac{1}{\bar{\alpha}}\nabla^2\right)w\right)&=\frac{dp}{dz}-\frac{\cos\alpha}{F}+G_rN_t\left(\frac{r^3-h^3}{18}\right)-G_r(N_b+N_t)\left(\frac{r^4-h^4}{64}\right)+G_rN_bN_t\left(\frac{r^5-h^5}{300}\right)-G_rN_bN_t\left(\frac{r^6-h^6}{1152}\right)\\&-B_r\left(\frac{r^2-h^2}{4}\right)\frac{N_t}{N_b}+B_r\left(\frac{r^2-h^2}{4}\right)\frac{N_t}{N_b}-B_r\frac{{N_t}^2}{N_b}\left(\frac{r^3-h^3}{18}\right)+B_r\frac{{N_t}^2}{N_b}\left(\frac{r^4-h^4}{64}\right)\end{aligned} \quad (25)$$

Solving Eq. (25) subject to the boundary conditions (14)- (17), the expression for velocity is given as

$$\begin{aligned}w=&-1+S_1\left(I_0(\bar{\alpha}r)-I_0(\bar{\alpha}h)\right)+\frac{dp}{dz}\left[\left(\left(\frac{\bar{\eta}-1}{2A}\right)\right)\left(I_0(\bar{\alpha}r)-I_0(\bar{\alpha}h)\right)+\frac{r^2-h^2}{4}\right]\\&-\frac{\cos\alpha}{F}\left[\left(\left(\frac{\bar{\eta}-1}{2A}\right)\right)\left(I_0(\bar{\alpha}r)-I_0(\bar{\alpha}h)\right)+\frac{r^2-h^2}{4}\right]\\&+G_rN_t\left[\frac{r^3-h^3}{18\bar{\alpha}^2}+\frac{r-h}{50\bar{\alpha}^4}+\frac{r^5}{450}-\frac{r^2h^3}{72}+\frac{7h^5}{600}\right]\\&+G_r(N_b+N_t)\left[\frac{r^4-h^4}{64\bar{\alpha}^2}+\frac{r^2-h^2}{4\bar{\alpha}^4}+\frac{r^4}{64\bar{\alpha}^2}-\frac{r^2h^4}{256}+\frac{r^6}{2304}+\frac{h^6}{288}\right]\\&+G_rN_bN_t\left[\frac{3(r-h)}{4\bar{\alpha}^6}+\frac{r^2-h^2}{2\bar{\alpha}^6}+\frac{r^3-h^3}{12\bar{\alpha}^4}-\frac{r^4-h^4}{32\bar{\alpha}^4}+\frac{r^5-h^5}{300\bar{\alpha}^2}-\frac{r^6-h^6}{1152\bar{\alpha}^2}-\frac{r^2h^5}{1200}+\frac{r^6}{14700}+\frac{r^2h^6}{4608}-\frac{r^8}{73728}-\frac{h^6}{14700}+\frac{h^7}{1200}-\frac{5h^8}{24576}\right]\\&+B_r\left(\frac{N_t}{N_b}-1\right)\left[\frac{r^2-h^2}{\bar{\alpha}^2}+\frac{r^4-h^4}{16}+\frac{r^2h^2}{16}\right]\\&+B_r\left(\frac{N_t^2}{N_b}\right)\left[-\frac{r-h}{2\bar{\alpha}^4}+\frac{3(r^2-h^2)}{2\bar{\alpha}^4}-\frac{r^3-h^3}{18\bar{\alpha}^2}+\frac{3(r^4-h^4)}{32\bar{\alpha}^2}+\frac{r^6-h^6}{384}+\frac{r^2h^3}{72}-\frac{r^5}{450}-\frac{r^2h^5}{256}-\frac{7h^5}{600}+\frac{h^7}{256}\right]\end{aligned} \quad (26)$$

where

$$A=\bar{\alpha}\left[\bar{\alpha}I_0(\bar{\alpha}h)-\left(\frac{1+\bar{\eta}}{h}\right)I_1(\bar{\alpha}h)\right] \text{and}$$

$$S_1 = -\frac{G_r N_t}{A}\left[\frac{-h^3}{36}(1+\bar{\eta}) + \frac{h}{3\bar{\alpha}^2}\left(1-\frac{\bar{\eta}}{2}\right) + \frac{2h^3}{45} - \frac{\bar{\eta}}{50\bar{\alpha}^4 h} - \frac{\bar{\eta}h^3}{90}\right] - \frac{G_r(N_b+N_t)}{A}\left[\frac{1}{2\bar{\alpha}^4} - \frac{\bar{\eta}}{2\bar{\alpha}^4} + \frac{h^4(1-\bar{\eta})}{192} + \frac{h^2(3-\bar{\eta})}{16\bar{\alpha}^2}\right] - \frac{G_r N_b N_t}{A}\left[\frac{h^5(\bar{\eta}-1)}{600} - \frac{(1+\bar{\eta})}{\bar{\alpha}^6} + \frac{h\left(1-\frac{\bar{\eta}}{2}\right)}{2\bar{\alpha}^4} + \frac{h^3\left(1-\frac{\bar{\eta}}{4}\right)}{15\bar{\alpha}^2} + \frac{h^4\left(1-\frac{\bar{\eta}}{5}\right)}{490} + \frac{h^6(1-\bar{\eta})}{2304} + \frac{h^2(\bar{\eta}-3)}{8\bar{\alpha}^4} + \frac{h^4(\bar{\eta}-5)}{192\bar{\alpha}^2} + \frac{h^6(\bar{\eta}-7)}{9216} - \frac{3\bar{\eta}}{4h\bar{\alpha}^6}\right] - \frac{B_r}{A}\left(\frac{N_t}{N_b}-1\right)\left[\frac{2(1-\bar{\eta})}{\bar{\alpha}^2} + \frac{h^2(1-\bar{\eta})}{8} + \frac{3h^2(1-\bar{\eta})}{4}\right] - \frac{B_r}{A}\frac{N_t^2}{N_b}\left[\frac{h^3(1-\bar{\eta})}{36} + \frac{h\left(-2+\frac{\bar{\eta}}{8}\right)}{6\bar{\alpha}^2} + \frac{h^3(\bar{\eta}+4)}{90} + \frac{3(1-\bar{\eta})}{\bar{\alpha}^4} + \frac{h^5(\bar{\eta}-1)}{128} + \frac{h^2(9-3\bar{\eta})}{8\bar{\alpha}^2} + \frac{h^4(5-\bar{\eta})}{64} + \frac{\bar{\eta}}{2h\bar{\alpha}^4}\right]$$

The dimension less flux in the moving frame is given as

$$q = \int_0^h 2rwdr \qquad (27)$$

Substituting Eq. (26) in Eq. (27) and solving, the flux is

$$q = -h^2 + 2S_1 S + \frac{dp}{dz}\left[\left(\left(\frac{\bar{\eta}-1}{A}\right)S\right) - \frac{h^4}{8}\right] - \frac{\cos\alpha}{F}\left[\left(\left(\frac{\bar{\eta}-1}{A}\right)S\right) - \frac{h^4}{8}\right] + G_r N_t\left[\frac{-h^5}{30\bar{\alpha}^2} - \frac{h^3}{150\bar{\alpha}^4} + \frac{3h^7}{560}\right] + G_r(N_b + N_t)\left[\frac{-h^6}{192\bar{\alpha}^2} - \frac{h^4}{8\bar{\alpha}^4} + \frac{5h^8}{3072}\right] + G_r N_b N_t\left[\frac{-h^3}{4\bar{\alpha}^6} + \frac{-h^4}{4\bar{\alpha}^6} - \frac{h^5}{20\bar{\alpha}^4} + \frac{h^6}{48\bar{\alpha}^4} + \frac{h^8}{1536\bar{\alpha}^2} + \frac{h^8}{19600} + \frac{h^9}{2400} - \frac{h^{10}}{10240}\right] + B_r\left(\frac{N_t}{N_b}-1\right)\left[\frac{-h^4}{2\bar{\alpha}^2} + \frac{5h^6}{96} - \frac{2h^7}{16}\right] + B_r\left(\frac{N_t^2}{N_b}\right)\left[\frac{-h^3}{\bar{\alpha}^4} - \frac{3(h^4)}{2\bar{\alpha}^4} + \frac{4h^5}{45\bar{\alpha}^2} - \frac{h^6}{16\bar{\alpha}^2} - \frac{3h^7}{360} - \frac{293h^8}{149376} + \frac{h^9}{512}\right] \qquad (28)$$

where $S = hI_1(\bar{\alpha}h) - \frac{h^2}{2}I_0(\bar{\alpha}h)$

From Eq. (28), the expression for $\frac{dp}{dz}$ is

$$\frac{dp}{dz} = \frac{-1}{S_0}q + \frac{\cos\alpha}{F} - \frac{h^2}{S_0} + \frac{2S_1 S}{S_0} + \frac{G_r N_t}{S_0}\left[\frac{-h^5}{30\bar{\alpha}^2} - \frac{h^3}{150\bar{\alpha}^4} + \frac{3h^7}{560}\right] + \frac{G_r(N_b+N_t)}{S_0}\left[\frac{-h^6}{192\bar{\alpha}^2} - \frac{h^4}{8\bar{\alpha}^4} + \frac{5h^8}{3072}\right] + \frac{G_r N_b N_t}{S_0}\left[\frac{-h^3}{4\bar{\alpha}^6} + \frac{-h^4}{4\bar{\alpha}^6} - \frac{h^5}{20\bar{\alpha}^4} + \frac{h^6}{48\bar{\alpha}^4} + \frac{h^8}{1536\bar{\alpha}^2} - \frac{h^8}{19600} + \frac{h^9}{2400} - \frac{h^{10}}{10240}\right] + \frac{B_r}{S_0}\left(\frac{N_t}{N_b}-1\right)\left[\frac{-h^4}{2\bar{\alpha}^2} + \frac{5h^6}{96} - \frac{2h^7}{16}\right] + \frac{B_r}{S_0}\left(\frac{N_t^2}{N_b}\right)\left[\frac{-h^3}{\bar{\alpha}^4} - \frac{3(h^4)}{2\bar{\alpha}^4} + \frac{4h^5}{45\bar{\alpha}^2} - \frac{h^6}{16\bar{\alpha}^2} - \frac{3h^7}{360} - \frac{293h^8}{149376} + \frac{h^9}{512}\right] \qquad (29)$$

where $S_0 = \frac{h^4}{8} - \left(\frac{\bar{\eta}-1}{A}\right)S$

The pressure drop over the wavelength $\Delta P_\lambda$ is defined as

$$\Delta P_\lambda = -\int_0^1 \frac{dP}{dz}dz. \qquad (30)$$

Substituting the expression $\frac{dp}{dz}$ in Eq. (30), the pressure drop is

$$\Delta P_\lambda = qL_1 + L_2 \qquad (31)$$

where $L_1 = \int_0^1 \frac{1}{S_0}dz$ (32)

and

$$L_2 = \int_0^1 \left(\frac{h^2}{S_0} - \frac{2S_1 S}{S_0} + \frac{\cos\alpha}{F} - \frac{G_r N_t}{S_0}\left[\frac{-h^5}{30\bar{\alpha}^2} - \frac{h^3}{150\bar{\alpha}^4} + \frac{3h^7}{560}\right] - \frac{G_r(N_b+N_t)}{S_0}\left[\frac{-h^6}{192\bar{\alpha}^2} - \frac{h^4}{8\bar{\alpha}^4} + \frac{5h^8}{3072}\right] - \frac{G_r N_b N_t}{S_0}\left[\frac{-h^3}{4\bar{\alpha}^6} + \frac{-h^4}{4\bar{\alpha}^6} - \frac{h^5}{20\bar{\alpha}^4} + \frac{h^6}{48\bar{\alpha}^4} + \frac{h^8}{1536\bar{\alpha}^2} - \frac{h^8}{19600} + \frac{h^9}{2400} - \frac{h^{10}}{10240}\right] - \frac{B_r}{S_0}\left(\frac{N_t}{N_b}-1\right)\left[\frac{-h^4}{2\bar{\alpha}^2} + \frac{5h^6}{96} - \frac{2h^7}{16}\right] - \frac{B_r}{S_0}\left(\frac{N_t^2}{N_b}\right)\left[\frac{-h^3}{\bar{\alpha}^4} - \frac{3(h^4)}{2\bar{\alpha}^4} + \frac{4h^5}{45\bar{\alpha}^2} - \frac{h^6}{16\bar{\alpha}^2} - \frac{3h^7}{360} - \frac{293h^8}{149376} + \frac{h^9}{512}\right]\right)dz \qquad (33)$$

Following the analysis of Shapiro et al.(1969), the time averaged flux over a period in the laboratory frame $\bar{Q}$ is given as

$$\bar{Q} = 1 + \frac{\epsilon^2}{2} + q \qquad (34)$$

Substituting Eq. (31) in equation Eq. (34), the time averaged flux is

$$\bar{Q} = 1 + \frac{\epsilon^2}{2} + \frac{\Delta P_\lambda}{L_1} - \frac{L_2}{L_1} \qquad (35)$$

The dimensionless frictional force $\bar{F}$ at the wall is

$$\bar{F} = \int_0^1 h^2\left(-\frac{dP}{dz}\right)dz \qquad (36)$$

**Heat Transfer Coefficient**

The heat transfer coefficient at the wall is given as

$$Z_\theta(r,z) = \left(\frac{\partial h}{\partial z}\right)\left(\frac{\partial \theta_t}{\partial r}\right) \quad (37)$$

**Mass Transfer Coefficient**

The mass transfer coefficient at the wall is as follows

$$Z_\sigma(r,z) = \left(\frac{\partial h}{\partial z}\right)\left(\frac{\partial \sigma}{\partial r}\right) \quad (38)$$

## 4. Results and Discussion

Analytical expressions for the pressure drop, time averaged flux, frictional force,heat transfer coefficient and mass transfer coefficienthave been calculated.Various graphs are depicted by using Mathematica software.

### 4.1 Pressure drop characteristics

Figs. 1.1-1.7 illustrate the variation of pressure drop $(\Delta p_\lambda)$with time averaged flux $(\bar{Q})$ of peristaltic waves for different values of couple-stress fluid parameters $\bar{\alpha}, \bar{\eta}$, Brownian motion parameter $(N_b)$, thermophoresis parameter $(N_t)$, local temperature Grashof number $(G_r)$, local nano particle Grashof number$(B_r)$ and inclination $(\alpha)$.

From Fig. 1.1, 1.3, 1.5 and 1.7 it is clear that pressure drop $(\Delta p_\lambda)$ increases with the couple-stress fluid parameter $\bar{\alpha}$, Brownian motion parameter $(N_b)$ ,local temperature Grashof number$(G_r)$and with inclination $(\alpha)$.It is observed from Fig 1.2 that pressure drop $(\Delta p_\lambda)$ increases with the couple-stress fluid parameter$\bar{\eta}$ in the peristaltic pumping region $(0 < \bar{Q} < 0.38)$ and decreases in the augmented pumping region $(0.42 < \bar{Q} < 1)$. From Figs. 1.4 &1.6, it is noticed that as the time averaged flux $(\bar{Q})$ increases, pressure drop $(\Delta p_\lambda)$ decreases with the increase of thermophoresis parameter $(N_t)$ and with the local nano particle Grashof number$(B_r)$.

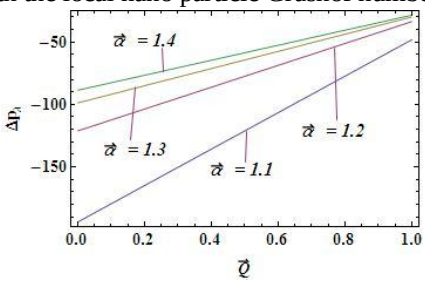


**Fig.1.1: Effect of $\bar{Q}$ and $\bar{\alpha}$ on $(\Delta p_\lambda)$**
$(\epsilon = 0.9, \bar{\eta} = 0.2, G_r = 0.5, B_r = 0.3, N_b = 1.3, N_t = 1.8, \alpha = 30^0)$

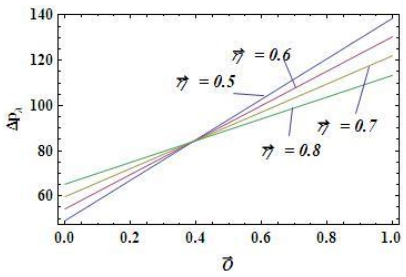


**Fig.1.2: Effect of $\bar{Q}$ and $\bar{\eta}$ on $(\Delta p_\lambda)$**
$(\epsilon = 0.4, \bar{\alpha} = 1, G_r = 0.5, B_r = 0.3, N_b = 1.3, N_t = 1.8, \alpha = 30^0)$

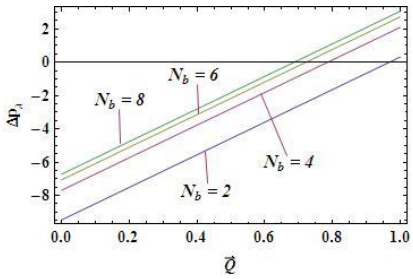


**Fig.1.3: Effect of $\bar{Q}$ and $N_b$on $(\Delta p_\lambda)$**
$(\epsilon = 0.1, \bar{\alpha} = 3.2, \bar{\eta} = 1.2, G_r = 0.5, B_r = 0.3, N_t = 1.8, \alpha = 30^0)$

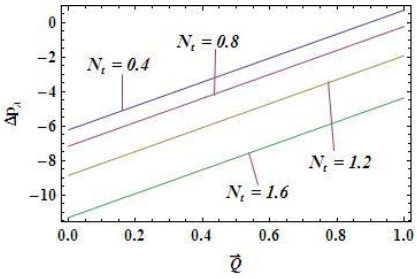


**Fig1.4: Effect of $\bar{Q}$ and $N_t$on $(\Delta p_\lambda)$**
$(\epsilon = 0.1, \bar{\alpha} = 1.2, \bar{\eta} = 0.8, G_r = 0.5, B_r = 0.3, N_b = 1.3, \alpha = 30^0)$

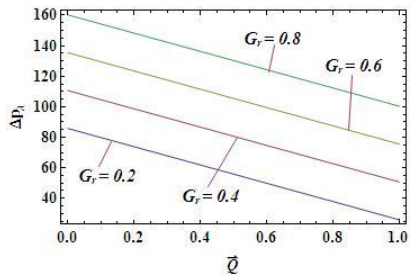


**Fig.1.5: Effect of $\bar{Q}$ and $G_r$on $(\Delta p_\lambda)$**
$(\epsilon = 0.3, \bar{\alpha} = 2.2, \bar{\eta} = 1.8, N_b = 1.3, B_r = 0.3, N_t = 1.8, \alpha = 30^0)$

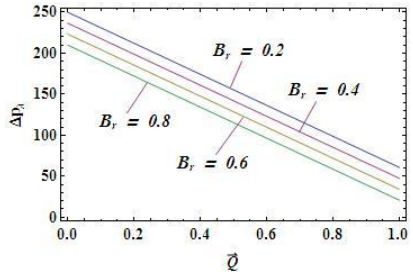


**Fig.1.6: Effect of $\bar{Q}$ and $B_r$on $(\Delta p_\lambda)$**
$(\epsilon = 0.9, \bar{\alpha} = 2.2, \bar{\eta} = 0.8, G_r = 0.5, N_b = 1.3, N_t = 1.8, \alpha = 30^0)$

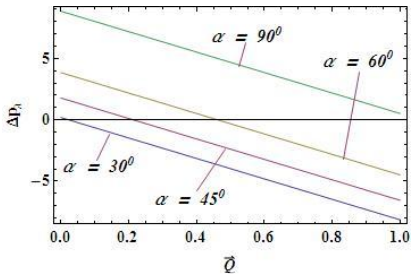


**Fig.1.7: Effect of $\bar{Q}$ and $\alpha$on $(\Delta p_\lambda)$**
**$(\epsilon = 0.9, \bar{\alpha} = 2.2, \bar{\eta} = 0.8, G_r = 0.5, N_b = 1.3, N_t = 1.8, B_r = 0.3)$**

## 4.2 Frictional Force

The variation of absolute value of the frictional force $(|\bar{F}|)$ with various parameters is shown graphically from Figs. 2.1-2.7. The frictional force $(|\bar{F}|)$ increases with couple-stress fluid parameter $\bar{\eta}$, thermophoresis parameter $(N_t)$ and with local Nano particle Grashof number $(B_r)$ but decreases withBrownian motion parameter $(N_b$ ),local temperature Grashof number $(G_r)$ and with inclination $(\alpha)$.

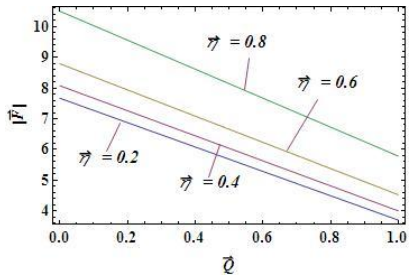


**Fig.2.1: Effect of $\bar{Q}$ and $\bar{\eta}$ on $\bar{F}$**
**$(\epsilon = 0.9, \bar{\alpha} = 1.8, G_r = 0.5, B_r = 0.3, N_b = 1.3, N_t = 1.8, \alpha = 30^0)$**

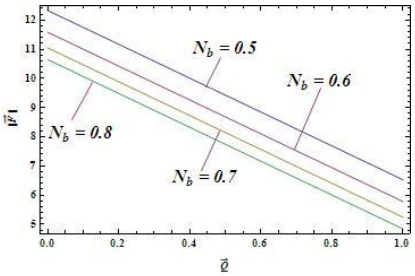


**Fig.2.2: Effect of $\bar{Q}$and$N_b$on $\bar{F}$**
**$(\epsilon = 0.5, \bar{\eta} = 0.2, G_r = 0.5, B_r = 0.3, \bar{\alpha} = 1.2, N_t = 1.8, \alpha = 30^0)$**

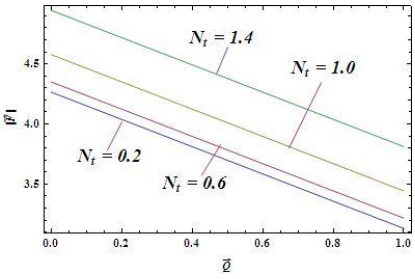


**Fig.2.3: Effect of $\bar{Q}$and$N_t$on $\bar{F}$**
**$(\epsilon = 0.5, \bar{\alpha} = 3.2, \bar{\eta} = 1.2, G_r = 0.5, B_r = 0.3, N_b = 1.3, \alpha = 30^0)$**

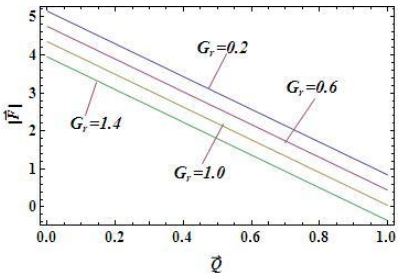


**Fig.2.4: Effect of $\bar{Q}$and $G_r$on $\bar{F}$**
**$(\epsilon = 0.1, \bar{\alpha} = 1.8, \bar{\eta} = 1.5, N_b = 1.3, B_r = 0.3, N_t = 1.8, \alpha = 30^0)$**

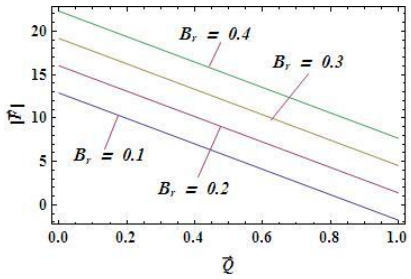


**Fig.2.5: Effect of $\bar{Q}$and $B_r$on $\bar{F}$**
**$(\epsilon = 0.1, \bar{\alpha} = 0.8, \bar{\eta} = 0.5, G_r = 0.5, N_b = 1.3, N_t = 1.8, \alpha = 30^0)$**

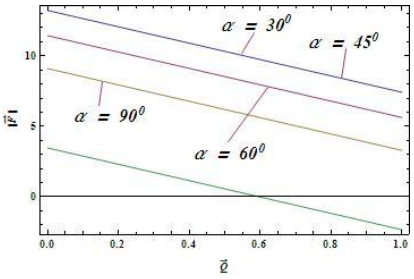


**Fig.2.6: Effect of $\bar{Q}$and$\alpha$ on $\bar{F}$**
**$(\epsilon = 0.1, \bar{\alpha} = 0.8, \bar{\eta} = 0.5, G_r = 0.5, N_b = 1.3, N_t = 1.8, B_r = 0.3)$**

## 4.3Temperature Profile

Effects of temperature profile $(\theta_t)$ with respect to the Brownian motion parameter $(N_b)$ and thermophoresis parameter $(N_t)$ has been shown from Figs. 4.1-4.2. It can be seen that, temperature profile $(\theta_t)$ increaseswith the increase of Brownian motion parameter $(N_b)$ and decreases with the increase of thermophoresis parameter $(N_t)$. It is interesting to observe that value of temperature profile $(\theta_t)$ is maximum in the range$[-0.5, 0.5]$.

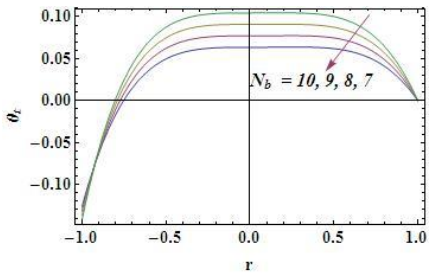


**Fig. 3.1: Variation in Temperature profile with $N_b$**
**$(z = 2, \epsilon = 0.1, N_t = 0.8)$**

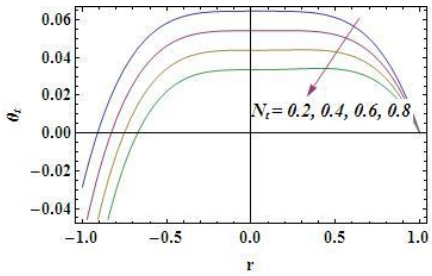


**Fig. 3.2: Variation in Temperature profile with $N_t$ $(z = 2, \epsilon = 0.1, N_b = 4.8)$**

## 4.4 Nanoparticle phenomena

Figs. 4.1-4.2 explain the nature of nanoparticle phenomena $(\sigma)$ for different values of Brownian motion parameter $(N_b)$ and thermophoresis parameter$(N_t)$. It can be seen that, the nano particle phenomena $(\sigma)$ increases with the increase of Brownian motion parameter $(N_b)$and decreases with the increase of thermophoresis parameter $(N_t)$. It is also observed that nano particle phenomena $(\sigma)$ attains maximum value at $r = 0$.

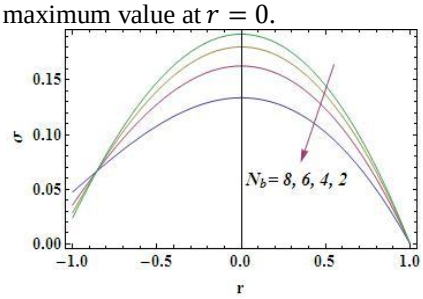


**Fig. 4.1: Variation in Nano particle with $N_b$ $(z = 2, \epsilon = 0.1, N_t = 0.8)$**

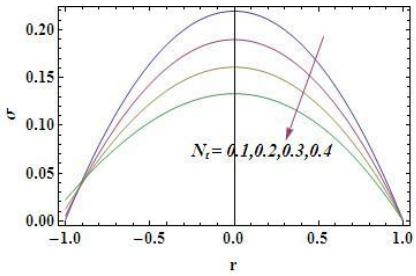


**Fig. 4.2: Variation in Nano particle with $N_t$ $(z = 2, \epsilon = 0.1, N_b = 0.3)$**

## 4.5 Heat Transfer Coefficient

Figs. 5.1-5.3 indicate the variation of heat transfer coefficient $(Z_\theta)$ for various values of Brownian motion parameter $(N_b)$, thermophoresis parameter $(N_t)$ and amplitude ratio $(\epsilon)$. From Figs. 5.1-5.3, it can be observed that, the value of the heat transfer coefficient $(Z_\theta)$ increases with Brownian motion parameter $(N_b)$ and thermophoresis parameter$(N_t)$,amplitude ratio $(\epsilon)$ and then decreases after attaining a constant value.

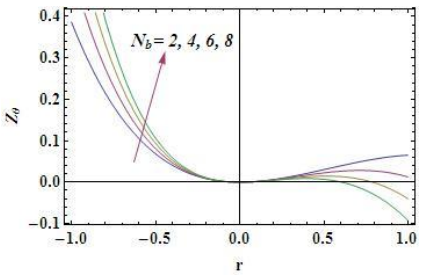


**Fig. 5.1: Variation in heat transfer coefficient with $N_b$ $(z = 2, \epsilon = 0.1, N_t = 1.8)$**

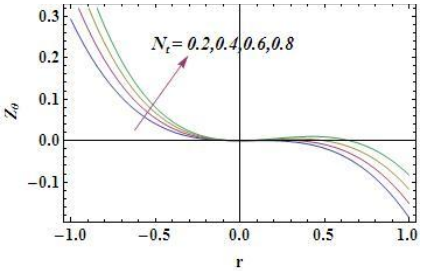


**Fig. 5.2: Variation in heat transfer coefficient with $N_t$ $(z = 2, \epsilon = 0.2, N_b = 2.8)$**

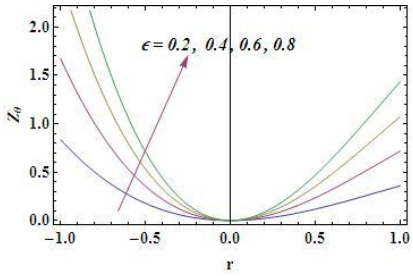


**Fig. 5.3: Variation in heat transfer coefficient with $\epsilon$ $(z= 2, N_t = 2.8, N_b = 0.2)$**

## 4.6 Mass Transfer Coefficient

Figs. 6.1-6.3 illustrate the effect of various parameters on mass transfer coefficient $(Z_\sigma)$. It is interesting to observe that, mass transfer coefficient $(Z_\sigma)$ increases with Brownian motion parameter $(N_b)$, thermophoresis parameter $(N_t)$ and with amplitude ratio $(\epsilon)$ and then decreases after attaining a constant value.

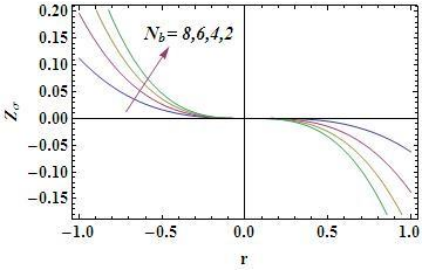


**Fig. 6.1: Variation in Mass transfer coefficient with $N_b$ $(z = 2, \epsilon = 0.1, N_t = 0.2)$**

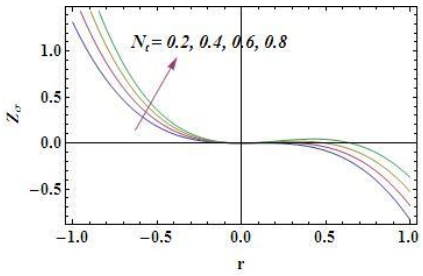


**Fig. 6.2: Variation in Mass transfer coefficient with $N_t$**
**$(z = 2, \epsilon = 0.9, N_b = 2.8)$**

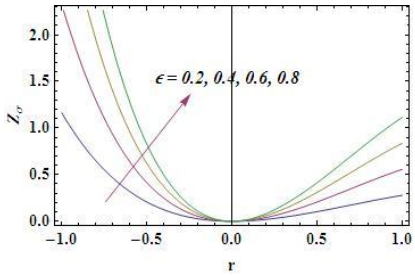


**Fig. 6.3: Variation in Mass transfer coefficient with $\epsilon$**
**$(z = 2, N_t = 2.8, N_b = 2.3)$**

### 4.7 Streamline patterns

Trapping is a phenomenon where the streamlines on the center line in the moving frame are divided in order to encircle a bolus of fluid particles circulating along closed streamlines under certain given conditions. Trapping is a characteristic of peristaltic motion. As the bolus emanate to be trapped by the wave, the bolus moves at equal speed with that of the wave.Figs. 7.1-7.4illustrates the streamline patterns and trapping for different values of couple-stress fluid parameters, Brownian motion parameter and local nano particle Grashof number.

From Fig. 7.1 it is clear that, the size of the trapped bolus decreases first and then increases with the increases of couple-stress fluid parameter $\bar{\alpha}$. It is observed from Fig. 7.2 that, the size of the trapped bolus increases with the increase of couple-stress fluid parameter $\bar{\eta}$ . From Fig. 7.3 it is noticed that, the size of the trapped bolus decreases with the increase of Brownian motion parameter ($N_b$). It is interesting to observe from Fig. 7.4 that, the size of the upper bolus increases and the size of the lower bolus decreases with the increase of local nanoparticle Grashof number ($B_r$).

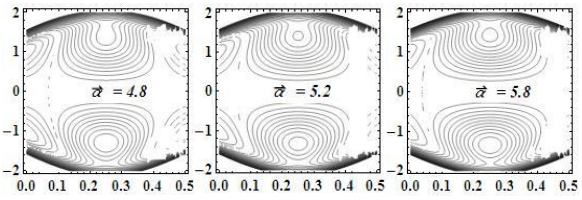


**Fig.7.1: Stream line patterns for different values of $\bar{\alpha}$**
**$(\epsilon = 0.5, \bar{Q} = 0.7, \bar{\eta} = 1.1, G_r = 6, B_r = 5, N_b = 10, N_t = 5, \alpha = 30^0)$**

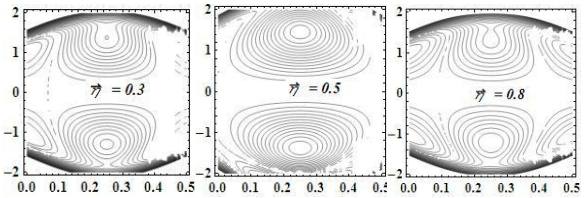


**Fig.7.2: Stream line patterns for different values of $\bar{\eta}$**
**$(\epsilon = 0.5, \bar{Q} = 0.7, \bar{\alpha} = 5, G_r = 6, B_r = 5, N_b = 10, N_t = 5, \alpha = 30^0)$**

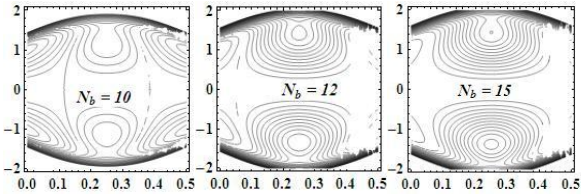


**Fig.7.3: Stream line patterns for different values of $N_b$**
**$(\epsilon = 0.5, \bar{Q} = 0.7, \quad \bar{\alpha} = 5, G_r = 6, B_r = 5, \bar{\eta} = 1.1, N_t = 5, \alpha = 30^0)$**

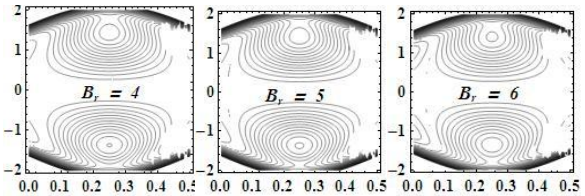


**Fig.7.4: Stream line patterns for different values of $B_r$**
**$(\epsilon = 0.5, \bar{Q} = 0.7, \quad \bar{\alpha} = 5, N_t = 5, G_r = 6, \bar{\eta} = 1.1, N_b = 10, \alpha = 30^0)$**

## 5 Conclusions

The major premise of the paper isPeristaltic transport of a couple-stress fluid with nanoparticles in an inclined tube with heat and mass transfer effects. The study particularly pertains to a situation when the Reynolds number is low and wavelength is large. Emphasis was laid to investigate the pressure drop characteristics, frictional force, temperature profile, nano particle phenomenon, heat transfer coefficient, mass transfer coefficient and streamline patternsof the couple-stress fluid parameters, Brownian motion parameter, thermophoresis parameter, local temperature Grashof number, local nano particle Grashof number and inclination. Homotopy perturbation method is used to solve the coupled equations of temperature profile and nano particle phenomena and analytical methods have been applied to the present study to find the other variables.

The main points of the analysis are as follows:

i Pressure drop increases with the couple-stress fluid parameter $\bar{\alpha}$, Brownian motion parameter, local temperature Grashof number and with inclination. Pressure drop increases with the couple-stress fluid parameter $\bar{\eta}$ in the peristaltic pumping region $(0 < \bar{Q} < 0.38)$ and decreases in the augmented pumping region $(0.42 < \bar{Q} < 1)$.

The absolute value of the frictional force $(|\bar{F}|)$ increases with couple-stress fluid parameter $\bar{\eta}$, thermophoresis parameter and with local Nano

particle Grashof number but decreases with Brownian motion parameter, local temperature Grashof number and with inclination.

iii Temperature profile increases with the increase of Brownian motion parameter and decreases with the increase of thermophoresis parameter. Value of temperature profileis maximum in the range$[-0.5, 0.5]$.

iv Nanoparticle phenomena $(\sigma)$ increases with the increase of Brownian motion parameter $(N_b)$and decreases with the increase of thermophoresis parameter $(N_t)$ and it attains maximum value at $r = 0$.

v Heat transfer coefficient increases with Brownian motion parameter and thermophoresis parameter, amplitude ratio $(\epsilon)$ and then decreases after attaining a constant value.

vi Mass transfer coefficient increases with Brownian motion parameter, thermophoresis parameter and with amplitude ratio and then decreases after attaining a constant value.

## REFERENCES


[1] Akbar, N. S., & Nadeem, S. (2013). Peristaltic flow of a micropolar fluid with nano particles in small intestine. *Applied Nanoscience*, *3*(6), 461–468.

[2] Das, S. K., Putra, N., & Roetzel, W. (2003). Pool boiling of nano-fluids on horizontal narrow tubes. *International Journal of Multiphase Flow*, *29*(8), 1237–1247. https://doi.org/10.1016/S0301-9322(03)00105-8

[3] Ellahi, R., Riaz, A., & Nadeem, S. (2014). A theoretical study of Prandtl nanofluid in a rectangular duct through peristaltic transport. *Applied Nanoscience*, *4*(6), 753–760. https://doi.org/10.1007/s13204-013-0255-4

[4] Fung, Y. C., & Yih, C. S. (1968). Peristaltic Transport. *Journal of Applied Mechanics*, *35*(4), 669–675. https://doi.org/10.1115/1.3601290

[5] Griffiths, D. (1989). Flow of urine through the ureter: a collapsible, muscular tube undergoing peristalsis. *Journal of Biomechanical Engineering*, *111*(3), 206–211.

[6] He, J.-H. (1998). Approximate analytical solution for seepage flow with fractional derivatives in porous media. *Computer Methods in Applied Mechanics and Engineering, Volume 167, Issues 1-2, 1 December 1998, Pages 57-68*. Retrieved from http://works.bepress.com/ji_huan_he/34

[7] Maiti, S., & Misra, J. (2012). Peristaltic transport of a couple stress fluid: some applications to hemodynamics. *Journal of Mechanics in Medicine and Biology*, *12*(03), 1250048.

[8] Maruthi Prasad, K., & Radhakrishnamacharya, G. (2008). Flow of Herschel–Bulkley fluid through an inclined tube of non-uniform cross-section with multiple stenoses. *Archives of Mechanics*, *60*(2), 161–172.

[9] Naby, A. E. H. A. El, & Shamy, I. El. (2007). Slip effects on peristaltic transport of power-law fluid through an inclined tube. *Applied Mathematical Sciences*, *1*(60), 2967–2980.

[10] Noreen, S. (2013). Mixed Convection Peristaltic Flow of Third Order Nanofluid with an Induced Magnetic Field. *PLoS ONE*, *8*(11), e78770. https://doi.org/10.1371/journal.pone.0078770

[11] Pal, D., Rudraiah, N., & Devanathan, R. (1988). A couple stress model of blood flow in the microcirculation. *Bulletin of Mathematical Biology*, *50*(4), 329–344.

[12] Prasad K., M., N., S., & M.A.S., S. (2015). Study of Peristaltic Motion of Nano Particles of a Micropolar Fluid with Heat and Mass Transfer Effect in an Inclined Tube. *International conference on computational heat and mass transfer (ICCHMT) - 2015*, *127*, 694–702. https://doi.org/10.1016/j.proeng.2015.11.368

[13] Prasad, K. M., & Radhakrishnamacharya, G. (2009). Effect of Peripheral Layer on Peristaltic Transport of a Couple Stress Fluid. *International Journal of Fluid Mechanics Research*, *36*(6), 573–583.

[14] Prasad, K. M., Radhakrishnamacharya, G., & Murthy, J. R. (2010). Peristaltic pumping of a micropolar fluid in an inclined tube. *Int. J. of Appl. Math and Mech*, *6*(11), 26–40.

[15] Prasad, K. M., Subadra, N., & Srinivas, M. (2015). Peristaltic Transport of a Nanofluid in an Inclined Tube. *American Journal of Computational and Applied Mathematics*, *5*(4), 117–128.

[16] Shapiro, A. H., Jaffrin, M. Y., & Weinberg, S. L. (1969a). Peristaltic pumping with long wavelengths at low Reynolds number. *Journal of Fluid Mechanics*, *37*(04), 799–825. https://doi.org/10.1017/S0022112069000899

[17] Shapiro, A. H., Jaffrin, M. Y., & Weinberg, S. L. (1969b). Peristaltic pumping with long wavelengths at low Reynolds number. *Journal of Fluid Mechanics*, *37*(04), 799–825. https://doi.org/10.1017/S0022112069000899

[18] Shit, G. C., & Roy, M. (2014). Hydromagnetic effect on inclined peristaltic flow of a couple stress fluid. *Alexandria Engineering Journal*, *53*(4), 949–958. https://doi.org/10.1016/j.aej.2014.07.007

[19] Srinivasacharya, D., Mishra, M., & Rao, A. R. (2003). Peristaltic pumping of a micropolar fluid in a tube. *Acta Mechanica*, *161*(3-4), 165–178.

[20] Stokes, V. K. (1966). Couple stresses in fluids. *Physics of Fluids (1958-1988)*, *9*(9), 1709–1715.

[21] S. U.S. Choi, J. A. E. (1995). Enhancing thermal conductivity of fluids with nanoparticles. ASME FED. *Proceedings of the ASME International Mechanical Engineering Congress and Exposition*, *66*.